Environ. Sci. Technol. **1999**, *33,* 1905−1910

Hydrodehalogenation of 1- to 3-Carbon Halogenated Organic Compounds in Water Using a Palladium Catalyst and Hydrogen Gas

GREGORY V. LOWRY AND MARTIN REINHARD*

Department of Civil and Environmental Engineering, Stanford University, Stanford, California 94305-4020

Supported palladium (Pd) metal catalysts along with H_2 gas show significant potential as a technology which can provide rapid, on-site destruction of halogenated groundwater contaminants. Pd catalyzes the rapid hydrodehalogenation of nine 1- to 3-carbon HOCs, resulting in little or no production of halogenated intermediates. Initial transformation rates were compared for 12 HOCs using 1 w/w% Pd-on-Al_2O_3 (Pd/Al) and metallic Pd catalysts in clean, aqueous batch systems at ambient pressure and temperature. Half-lives of 4−6 min were observed for 5−100 μM (1−10 mg/L) aqueous concentrations of PCE, TCE, *cis*-, *trans*-, 1,1-DCE, carbon tetrachloride, and 1,2-dibromo-3-chloropropane at ambient temperature and pressure with 0.22 g/L of catalyst. Using Pd/Al, TCE transformed quantitatively (97%) to ethane without formation of any detectable chlorinated intermediate compounds. This implies a direct conversion of TCE to ethane at the Pd surface. Carbon tetrachloride transformed primarily to methane and ethane and minor amounts of ethylene, propane, and propylene. Chloroform is a reactive intermediate (20%). Formation of C2 and C3 products implies a free radical mechanism. Methylene chloride, 1,1-dichloroethane, and 1,2-dichloroethane were nonreactive. Reaction mechanisms and kinetic models are postulated for TCE, carbon tetrachloride, and chloroform transformation.

Introduction

The widespread contamination of groundwater by chlorinated solvents and pesticides is a well-known environmental problem. Current treatment methods, such as air stripping, carbon absorption, and bioreactors, are limited in that they may (i) transfer contaminants from one medium to another and require further treatment prior to disposal, (ii) lead to the production of lesser chlorinated products which may be more toxic than the parent compound, and (iii) are often not effective on the entire range of contaminants at a site. As a result of these inadequacies, treatment technologies which provide on-site destruction of a wide range of HOCs in water at ambient conditions are needed.

The use of elemental iron for reductive dechlorination and nitrate removal has recently emerged in the literature (*1*−*4*) but is limited by slow rates, the gradual consumption of iron, and accumulation of toxic products in some cases. For example, carbon tetrachloride is readily converted to chloroform and more slowly to methylene chloride (MeCl), but the reaction essentially stops there and MeCl accumulates (*2*). The destruction of HOCs in water at mild or ambient conditions using noble metal catalysts and H_2 gas (*5*−*7*), or palladized iron (*8*), has recently afforded some attention in the literature. Also, noble metal catalysts are effective for the destruction of halogenated aromatics (1,2-dichlorobenzene), chlorinated biphenyls (4-chlorobiphenyl), and hydrogenation of polyaromatic hydrocarbons (PAH's) at ambient conditions in hydrogen saturated water (*9*).

SCHEME 1. Sequential and Direct Reaction Pathways for Conversion of TCE to Ethane

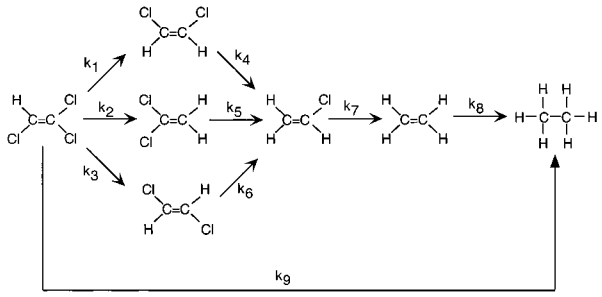

The palladium catalyzed reactions studied are hydrodehalogenation and hydrogenation. If complete, these reactions yield saturated hydrocarbons that are of little or no health concern. Details of these reactions are given elsewhere (*6, 7, 10*−*12*). As an example, in the absence of byproduct formation, the hydrodehalogenation and hydrogenation of trichloroethylene (TCE) can be hypothesized as in Scheme 1. Palladium catalyzes the hydrodehalogenation reactions, k_1−k_7, in which chlorine atoms are removed and replaced with hydrogen atoms, along with the formation of HCl. The double bond is also hydrogenated to yield ethane (k_8). Distinguishing between a sequential pathway through lesser chlorinated compounds or a direct pathway to ethane (k_9) is important for assessing the potential formation of toxic intermediates. Although reported studies (*4*−*9*) have shown the potential of palladium catalysts for treating contaminated aqueous waste streams at ambient temperature and pressure, few have addressed the potential formation of toxic intermediates and products or the details of the hydrodehalogenation pathway such as radical formation, final product distribution, and catalyst support effects.

A demonstration of the applicability of palladium metal catalysts for the destruction of several HOCs was performed in clean, aqueous batch systems. Initial rates measured in a zero-headspace reactor are used to compare the relative reactivity of 11 HOCs, and conclusions are drawn regarding structure and reactivity. Experiments with TCE, carbon tetrachloride (CT), chloroform (CF), and methylene chloride (MeCl) in headspace reactors are used to (i) elucidate mechanistic differences in transformation of chlorinated ethylenes and chlorinated methanes, (ii) assess the potential for toxic intermediate formation, and (iii) determine product distributions. Mathematical models and reaction pathways are postulated. Supported and unsupported palladium catalysts are used to investigate how the catalyst support affects the potential formation of halogenated intermediate compounds.

* Corresponding author phone: (650)723-0308; fax: (650)723-7058; e-mail: reinhard@ce.stanford.edu.

DOI:10.1021/es980963m CCC: $18.00 Published on Web 04/15/1999

TABLE 1. Catalyst Physical Properties

physical properties	Pd-met	Pd/Al
av particle size (μm)	0.25−0.55	38−70
Pd content (% w/w)	99.95	1
BET surf. area (m^2/g)	5	155
pore volume (cm^3/g)	0.01	0.20
pore size dist (nm)	nonporous	<8 (78%), 20−80 (8%)
metal dispersion (%)	N/A	21

TABLE 2. Reactor Operating Conditions

	zero-HS reactor	HS reactor
temp (K)	294 ± 1	295 ± 0.2
pressure (atm)	1	1.20−1.34
$[H_2]_{aq}$ (μM)[a]	800	960−1070
vol. (L)	1.15	2.0
aq/vap	1.15/0.0	1.5/0.5
pH		
initial	6.5−6.8	6.6−6.8
final	4.0−5.0	3.0−4.0
agitator speed (rpm)	500	1000
C_{cat} (g/L)	0.22	0.05−0.34[b]
$[HOC]_o$ (μM)	5−100	25−250

[a] $[H_2]_{aq}$ estimated using Henry's constant ($K_H = 7 \times 10^4$ atm). [b] Catalyst concentration was adjusted to keep experimental times under 6 h.

Experimental Section

Chemicals. Twelve halogenated organic compounds (RX) were studied. All reagents were 99+% pure unless noted. Tetrachloroethylene (PCE), 1,1-dichloroethylene (DCE), *cis*-DCE (97%), *trans*-DCE (98%), 1,2-dichloroethane (DCA), and 1,1,2-trichlorotrifluoroethane (Freon-113) were supplied by Aldrich. TCE was supplied by Fisher. CT and MeCl were supplied by J. T. Baker. The 1,1-DCA was supplied by Suppelco. The 1,2-dibromo-3-chloropropane (DBCP, 97%) was supplied by Pfaltz and Baur, and CF was supplied by Mallinckrodt. All compounds were used as received without further purification.

Catalysts. The Pd-on-Al_2O_3 (Pd/Al) (Aldrich) and metallic palladium (Pd-met) (Alfa Aesar) catalysts were supplied and used in a prereduced powdered form. No special precautions were taken to avoid catalyst exposure to air prior to kinetic experiments. Catalyst physical properties are given in Table 1. BET surface area, pore volume, and pore size distribution were measured using a Coulter SA 3100 surface area and pore size analyzer. Particle size distributions were determined with a Coulter LS 230 laser diffraction particle size analyzer. Metal dispersion (percent of metal available for catalysis) for the supported catalyst was determined by a commercial laboratory (Coulter, Particle Characterization Division). The 1 wt % palladium content of the Pd/Al catalyst specified by the manufacturer was assumed to be accurate.

Zero-Headspace Reactors. The zero-headspace reactor was a 1.15-L glass reactor equipped with two sample ports. Reactor operating conditions are given in Table 2. The experimental procedure for the zero-headspace reactors was as follows. The reactor was filled with Milli-Q water and 0.25 g of the Pd/Al catalyst was added**.** The reactor was then sparged with pure H_2 gas for 15 min to remove dissolved oxygen (reactive species) and provide an excess of hydrogen (est. 800 μM). DO was measured with a Hansatech DW1 oxygen electrode and found to be less than 0.15 mg/L after sparging. After sparging, a concentrated aqueous solution of known contaminant concentration was quickly added to provide initial contaminant concentrations of 5−100 μM (1−10 mg/L). One-milliliter samples were withdrawn from the reactor (displaced by H_2 saturated water to maintain zero headspace) and extracted into 0.5 mL of hexane or toluene.

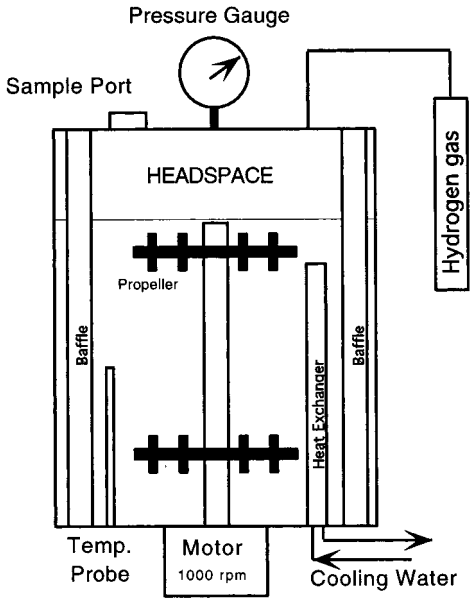

FIGURE 1. Headspace reactor. Total reactor volume is 2 L with 1.5 L of liquid and 0.5 L of headspace.

Replicate 1-μL samples of the extract were analyzed for the parent compound and chlorinated intermediates using a HP 5890 series II GC equipped with an electron capture detector and a 30 m × 0.32 mm i.d. DB-1701 capillary column (J&W). Nonhalogenated products were not measured in the zero-headspace experiments. The instrument was calibrated daily using standards prepared from volumetric dilutions of a stock solution. The water was unbuffered in all experiments. As a result of the hydrodehalogenation reactions the reactor pH decreased from an initial value of 6.5−6.8 to 4−5.

Headspace Reactors. The headspace reactor was a gastight 2.0-L glass and stainless steel reactor (Bioengineering AG, Wald, Switzerland) equipped with a magnetically driven mixer, temperature probe, heat exchanger, and pressure gauge (Figure 1). Two 5-cm impellers and four 2-cm baffles at the outer edge provide ample mixing. The impeller speed and reactor temperature were monitored and controlled by an attached computer. Reactor operating conditions are given in Table 2.

The experimental procedure for the headspace reactor was similar to that of the zero-headspace reactor except that (i) headspace was present, (ii) the reactor was kept under a constant hydrogen pressure (1.2−1.3 atm) throughout the experiment, and (iii) the catalyst was added last, after the contaminant had equilibrated between the aqueous and vapor phases. Headspace samples (200 μL) were withdrawn from the reactor and analyzed by GC using methods adapted from Burris et al. (*13*). Samples were injected splitless at 225 °C onto a HP 5890 GC equipped with a 30-m megabore GSQ-PLOT column (J&W) and a FID detector. The oven temperature profile was 50 °C for 2 min, ramp 40 °C/min to 220 °C, and hold at 220 C for 2 min. This method provided excellent resolution for the parent compounds, all chlorinated intermediates, and the C1−C3 hydrocarbon products in a single run. Detection limits using this method were TCE 0.2 μM, 1,1-DCE 0.1 μM, *cis*-DCE 0.1 μM, *trans*-DCE 0.1 μM, CT 1.0 μM, and CF 2.5 μM. HOC standards (except vinyl chloride) were prepared as described above, and calibration factors were calculated based on the total amount of compound added to the bottle (25% hs/75% aq). Nonhalogenated gas standards and vinyl chloride were purchased from Scott Specialty Gases.

Mass Transfer Limitations. Liquid−solid, gas−liquid, and intraparticle mass transfer limitations were considered. The

overall liquid−solid mass transfer rate constant, $K_{ls}a$, was estimated using the slip velocity approach of Harriott (*14*). $K_{ls}a$ was 4−5 orders of magnitude larger than the largest reaction rate constant, indicating that liquid−solid mass transfer resistance is negligible. This is primarily because the catalyst particles are small ($d_p < 100\ \mu$m) and the mixing rates are rapid.

The overall gas−liquid mass transfer rate constant, $K_{lg}a$ (applicable in the headspace reactors), was estimated based on the results of Roberts and Dandliker who studied mass transfer of VOCs from aqueous solution to the atmosphere during surface aeration (*15*). $K_{lg}a$ values in a similar system were determined for various power inputs. Based on these results, it is estimated that $K_{lg}a$ values in the headspace reactor are approximately 7−10 times larger than the observed reaction rate constants using Pd/Al and three times larger than the observed reaction rate constants using metallic palladium. Therefore, gas−liquid mass transfer resistance may have slowed the absolute reaction rates approximately 14−33% for the fastest reacting compounds. However, kinetic pathways and final product distributions are relatively unaffected, because the reactions are first order with respect to the HOCs and the rate constants should not change.

Intraparticle mass transfer limitations, applicable to the Pd/Al catalyst, were estimated using the method of Weisz and Prater (*16*) which requires only the observed reaction rate constant and catalyst properties: particle diameter (d_p) and effective diffusivity (D_e). In all cases, the ratio of intraparticle diffusion and reaction time scales, $k_{obs}d^2_p/D_e$, was 0.1 or less, indicating that intraparticle mass transfer resistance is minimal.

Evaluation of Reaction Kinetics. Transformation kinetics in the zero-headspace reactor were modeled with a simple pseudo-first-order rate law (eq 1)

$$-\frac{1}{C_{cat}}\frac{dC_a}{dt} = k_{obs}C_a \qquad (1)$$

where C_a and C_{cat} represent the HOC and catalyst concentration, respectively, and k_{obs} is the observed pseudo-first-order reaction rate constant. To correct for variances in catalyst concentration between experiments, the observed reaction rate constants are normalized by the catalyst concentration, such that the reported reaction rate constants, k_{rxn}, have units L g_{cat}^{-1} min^{-1}. It is presumed that the reaction rate is directly proportional to the catalyst concentration over the range of catalyst concentrations used. Hydrogen is not included in the rate expression, as the rates were found to be independent of the H_2 concentration under the conditions used (data not shown). This is because the activation energy for H_2 chemisorption on noble metals is close to zero such that the rates of adsorption and desorption of H_2 onto catalyst sites are sufficiently high (*17*), and because the aqueous H_2 concentration remains high (zero-headspace experiments) or constant (headspace experiments) throughout each experiment. Observed pseudo-first-order rate constants for zero-headspace experiments were calculated from linear regressions of $\ln\{[C_a]_t/[C_{ao}]\}$ vs time and normalized by the catalyst concentration to directly compare the results from individual experiments. Kinetic data from the headspace reactor were evaluated using a kinetic modeling software package, Scientist v. 2.01 (MicroMath) as described below.

Results and Discussion

Zero-Headspace Reactor Results. Initial rate data were determined from the disappearance of contaminant from solution. The initial concentration, normalized pseudo-first-order rate constant, and reactor specific half-life are given in Table 3. The hydrodehalogenation rates for the chlorinated ethylenes, CT, and DBCP are extremely rapid, with half-lives between 3.8 and 5.9 min at a Pd/Al concentration of 0.22 g/L. Exceptions are chloroform ($t_{1/2}$ = 73.3 min), Freon-113 ($t_{1/2}$ = 21.0 min), and the dichloroethanes, which showed very little reactivity even at elevated catalyst concentrations. Trace amounts of ethane were observed in DCA experiments (measured in a headspace experiment, data not shown), suggesting that dechlorination may occur, but no reduction in DCA concentration was evident after 24 h. No detectable levels of chlorinated intermediates or products (>0.1 μM) resulted from transformation of the chlorinated ethylenes and DBCP when the Pd/Al catalyst was used. Chloroform was produced as a reactive intermediate during the transformation of CT, accounting for about 20% of the initial CT at the maximum, but no methylene chloride or chloromethane was detected.

TABLE 3. HOC Transformation Rate Constants and Half Lives in Zero-HS Reactor Using Pd/Al

RX	$[HOC]_o$ (μM)	k_{rxn} (L g_{cat}^{-1} min^{-1})	R^2	$t_{1/2}$ (min)
Ethylenes				
PCE	7.8	0.53	0.976	5.9
TCE	22.8	0.64	0.993	4.9
1,1-DCE	23.7	0.70	0.997	4.5
cis-DCE	76.3	0.83	0.996	3.8
trans-DCE	75.3	0.78	0.997	4.0
Methanes				
CT	4.6	0.58	0.998	5.4
CF	35.2	0.04	0.989	73.3
Ethane/Propane				
Freon-113	21.3	0.15	0.999	21.0
DBCP	18.2	0.62	0.997	5.1
1,1-DCA	101	0		
1,2-DCA	101	0		

The disparity in reactivity between Freon-113, 1,1-DCA, DBCP, and 1,2-DCA is of interest because it may correlate with their structure. Freon-113 (ClF_2CCCl_2F) is reactive but 1,1-DCA (H_3CCCl_2H) is not, and DBCP ($H_2BrCH_2BrCCClH_2$) is reactive while 1,2-DCA ($H_2ClCCClH_2$) is not. This may be because the C−X bond dissociation energy decreases with increasing number of halogen atoms, and the fact that the ease of reductive dehalogenation generally follows the order I > Br > Cl ≫ F (*18*). Interestingly, minor differences in reactivity of the chlorinated ethylenes ($k_{DCE} > k_{TCE} > k_{PCE}$) contradicts the expected values based on bond dissociation energies. Reasons for this trend are unclear at this time.

Headspace Reactor Results. Initial contaminant concentrations and normalized pseudo-first-order rate constants determined from mechanistically derived model fits of kinetic data are given in Table 4. A mechanism was assumed in each case based on the formation of products and intermediates (or lack thereof), and the models described by a set of ordinary differential equations (eqs 2−6). Rate constants were then determined from the least-squares fitting procedure incorporated in the Scientist software package. Rate constant subscripts coincide with a specific reaction pathway as shown in Scheme 1 and Figure 5. Reaction intermediates and product distributions measured at the termination of each experiment are presented in Table 5.

1. Trichloroethylene Transformation Using the Pd/Al Catalyst. TCE transformation using the Pd/Al catalyst is shown in Figure 2a. Transformation of TCE yielded ethane as the only reaction product. Minor amounts of ethylene were formed (<1% data not shown), but no chlorinated intermediates were detected (<0.1 μM). A carbon mass balance of 97% was achieved in the system, providing

TABLE 4. Transformation Rate Constants for TCE, CT, and CF in Headspace Reactor

RX	$[HOC]_o$ (μM)	cat	C_{cat} (g/L)	k_{rxn}[a] (L g_{cat}^{-1} min^{-1})
TCE	25.3	Pd/Al	0.047	$k_9 = 0.34 \pm 0.02$
TCE	250	Pd-met	0.017	$k_9 = 4.4 \pm 0.5$
				$k_{loss} = 0.7 \pm 0.2$
CT	57.3	Pd/Al	0.067	$k_{10} = 0.15 \pm 0.01$
				$k_{11} = 0.02 \pm 0.005$
				$k_{12} = 0.06 \pm 0.008$
				$k_{13} = 0.01 \pm 0.01$
CT	47.3	Pd-met	0.026	$k_{10} = 1.5 \pm 0.3$
				$k_{11} = 0.4 \pm 0.15$
				$k_{12} = 1.0 \pm 0.3$
				$k_{13} = 0.1 \pm 0.15$
CF	53.3	Pd/Al	0.336	$k_{13} = 0.014 \pm 0.002$

[a] Errors are 95% confidence intervals.

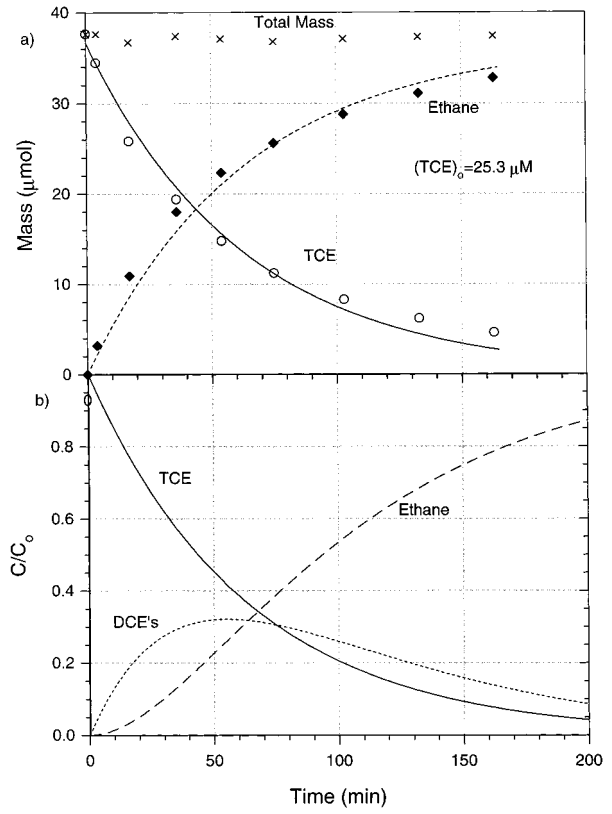

FIGURE 2. (a) Transformation of TCE in headspace reactor using 0.047 g/L Pd/Al. Lines represent first-order model fit (eq 2) for direct conversion of TCE to ethane. A 97% carbon mass balance was achieved. (b) Simulation of TCE transformation and expected production of DCE isomers if TCE transformation was a sequential reductive dechlorination through DCE.

evidence that chlorinated intermediates did not accumulate in the system.

TCE transformation data were fitted using a simple pseudo-first-order model for the complete conversion of TCE to ethane at the catalyst surface (eq 2)

$$-\frac{dC_{TCE}}{dt} = \frac{dC_{ethane}}{dt} = k_9 C_{TCE} \qquad (2)$$

and are shown as lines in Figure 2a. Some deviation from pseudo-first-order behavior is evident, as the model slightly under predicts TCE transformation at early times and over predicts TCE transformation at later times. This may be due

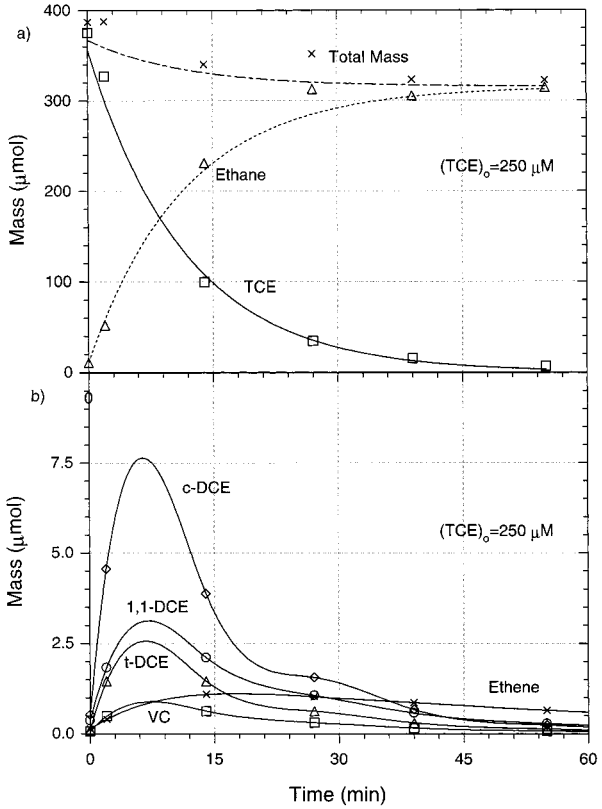

FIGURE 3. (a) Transformation of TCE in headspace reactor using 0.017 g/L of metallic palladium. Lines represent first-order model fit (eq 2) for direct conversion of TCE to ethane with an additional term (k_{loss}) accounting for the lost mass. An 83% carbon mass balance was achieved. (b) Production and decay of DCE isomers, VC, and ethylene. Total chlorinated intermediates account for 3−4% of initial TCE at their maximum. Lines in Figure 3b are interpolated (not fit) and only meant to guide the eye.

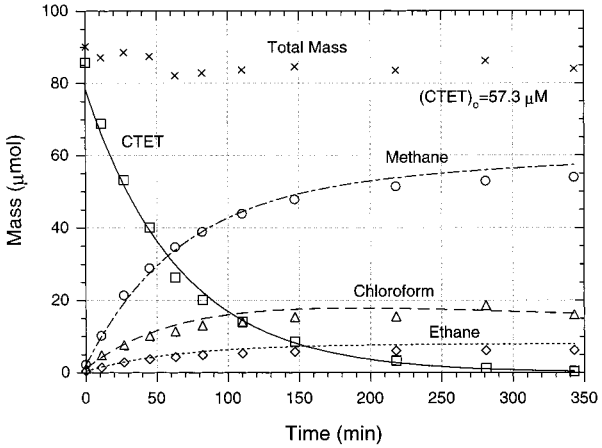

FIGURE 4. Carbon tetrachloride transformation using 0.067 g/L Pd/Al. Lines represent first-order model fit (eqs 3−6) with chloroform as a reactive intermediate. A 92% carbon mass balance was achieved.

to a decrease in catalyst activity over the course of the experiment. In general, this simple model provides a good fit of the data, and the formation of ethane is coincident with TCE disappearance.

The complete conversion of TCE to ethane at the catalyst surface contrasts the sequential reductive dechlorination, TCE to DCE to VC and finally to ethylene, evident in many anaerobic biological cultures (*19*), but is similar to TCE conversion observed in some zero-valent iron systems (*20*).

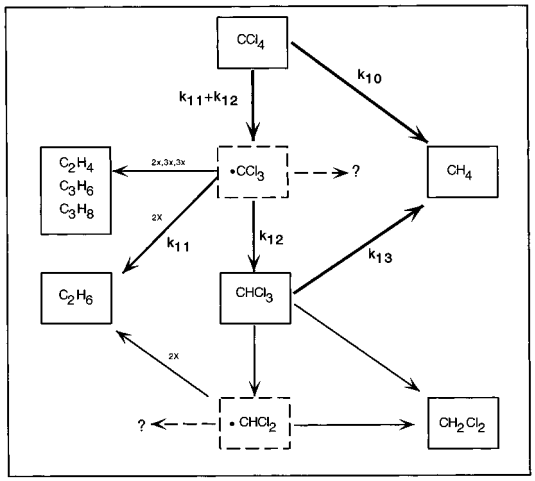

FIGURE 5. Proposed reaction pathways for transformation of carbon tetrachloride and chloroform. Solid boxes represent observed products and intermediates, and dashed boxes represent hypothesized intermediates.

TABLE 5. Product Distributions for TCE, CT, and CF Transformation in Headspace Reactor

RX/cat	intermediates (% max)	expt duration (min)	products/inter. at expt termntn (%)	carbon M.B. (%)
TCE/Pd/Al	ethylene (<1)	163	ethane (97) ethylene (<1)	97
TCE/Pd-met	ethylene (<1) 1,1-DCE (<1) *cis*-DCE (2) *trans*-DCE (<1) VC (<1)	193	ethane (83) unknown 1 (?) unknown 2 (?)	83
CT/Pd/Al	CF (21) ethylene (<1) propylene (trace)	343	methane (60) CF (18) ethane (14) propane (1.0)	92
CT/Pd-met	CF (24) ethylene (trace) propylene (trace)	113	methane (51) CF (23) ethane (12) propane (2)	88
CF/Pd/Al		291	methane (80) ethane (<1) MeCl (trace)	81

Complete conversion of TCE to ethane at the catalyst surface can be further corroborated with a simulation of the expected transient DCE concentrations (Figure 2b) based on the independently measured transformation rates for TCE and DCE (k_{tce} = 0.34 L g^{-1} min^{-1}, k_{dce} = 0.44 L g^{-1} min^{-1}). TCE transformation to the three DCE isomers (cis, trans, and 1,1) is assumed to be stoichiometric and considered together such that the DCE concentration is a sum of the three individual isomers. The DCE transformation rate constant used is that of *cis*-DCE as this was the most rapid and would yield the minimum expected transient total DCE concentration if TCE were to transform sequentially through DCE. Transient production of VC and ethylene are not included in the simulation. These compounds were not tested in this study but have been shown to rapidly transform to ethane via similar mechanisms in other studies (*7*, *12*). It is apparent from the simulation that a substantial amount of total DCE (32% at max) should appear if the hydrodehalogenation reaction were sequential. Coincident ethane formation, the lack of any detectable halogenated intermediates, and good carbon mass balances are evidence that a complete conversion of TCE to ethane occurs at the catalyst surface.

The lack of chlorinated intermediates is an advantage when considering the use of palladium catalysts for treatment of contaminated water but may be due to effects of the alumina support, as activity and selectivity of heterogeneous catalysts are commonly affected by the support material (*21*, *22*). Also, adsorption of chlorinated intermediates (DCEs and VC) on the support may be suppressing detection of these compounds. Experiments were performed using metallic palladium powder to investigate whether the support suppresses production of chlorinated intermediates.

2. Trichloroethylene Transformation Using Metallic Palladium. TCE transformation using pure palladium powder is shown in Figure 3a. Equation 2 was used to fit the data with an additional first-order rate constant k_{loss} added to account for the lost mass in the system. The normalized pseudo-first-order rate constants, k_9 and k_{loss}, are given in Table 4. TCE transformation again resulted in the simultaneous generation of ethane as the primary product, but Figure 3b shows that all three DCE isomers, VC, and ethylene were also formed. The total maximum concentration of chlorinated intermediates (DCEs + VC) was low and never exceeded 3−4% of the initial TCE. Interestingly, the three DCE isomers and VC appear in the system simultaneously, reach their maximum concentrations in the first 8 or 9 min, and continue to hydrodehalogenate even though TCE is present at concentrations 100 times greater. The formation of DCE and VC appears to be a transient phenomena occurring only in the first few minutes of the reaction.

The carbon mass balance of 83% is lower than the 97% achieved with the Pd/Al catalyst. There were two unidentified peaks in the chromatogram with a retention time between VC and 1,1-DCE that appeared to represent stable products. An attempt to identify these products based on retention time in GC analysis was unsuccessful, but it was determined that these products are not butane or hexane, which have been shown to be final products in the transformation of TCE by palladized iron (*8*). The low levels of transient chlorinated intermediates are further evidence that the predominant transformation mechanism is via complete transformation of TCE to ethane at the palladium surface, but the fact that they are produced in the system indicates the potential accumulation of these unwanted halogenated intermediates in a treatment system if the catalyst characteristics change.

3. Carbon Tetrachloride, Chloroform, and Methylene Chloride Transformation Using Pd/Al. Carbon tetrachloride transformation using the Pd/Al catalyst is shown in Figure 4. CT transformation results primarily in the formation of methane (60%), but chloroform is a reactive intermediate accounting for as much as 21% of the initial CT. No methylene chloride or chloromethane was detected. A total carbon mass balance of 92% was achieved in the system. Figure 4 also reveals that a substantial amount of ethane was produced, accounting for 14% of initial CT. Minor amounts of ethylene, propylene, and propane were also produced in the system (Table 5).

Chloroform transformation using the Pd/Al catalyst yielded methane as the primary reaction product (80%). Trace amounts of ethane (<1% of initial CF) and methylene chloride (not quantifiable) were detected (Table 5). Although chloroform transformation is 15−20 times slower than that of carbon tetrachloride (Table 4), 66% transformation of chloroform was achieved in 291 min with 0.33 g/L Pd/Al.

Methylene chloride showed virtually no reactivity when using the Pd/Al catalyst. No decrease in methylene chloride concentration was evident, and only trace levels of methane were detected in the reactor after 78 min, even at elevated catalyst concentrations. This contrasts results of Muftikian et al. (*8*), where a 75% reduction of methylene chloride was observed in a system with 3.6 g of palladized iron in 10 mL

of a 200 mg/L methylene chloride solution, but is similar to results with iron metal alone which showed very little methylene chloride transformation after several months (*2*).

4. Carbon Tetrachloride Transformation Using Metallic Palladium. Carbon tetrachloride transformation using metallic palladium resulted in a nearly identical product distribution as with Pd/Al (Table 5). The carbon mass balance of 88% was similar to that achieved with Pd/Al. This result reveals that palladium metal is indeed responsible for the transformation, and the alumina support appears to have little effect on the transformation of carbon tetrachloride.

5. Proposed Reaction Pathway and Kinetic Model for Carbon Tetrachloride and Chloroform. Based on observed reaction products and intermediates, hypothesized reaction pathways for the transformation of CT and chloroform are shown in Figure 5. Carbon tetrachloride transforms in part via a direct pathway to methane (k_{10}), but production of C2 and C3 hydrocarbons implies that CT transformation also occurs in part via production of a radical species ($k_{11} + k_{12}$). Trichloromethyl radical formation is most likely and may account for the formation of chloroform (k_{12}), as this pathway has been observed in biotic and abiotic transformations of CT in aqueous systems (*23*−*25*).

Chloroform transforms predominantly via a direct conversion to methane (k_{13}) because only trace amounts of radical coupling products (ethane) were observed, and there was no accumulation of the nonreactive species methylene chloride. A single reduction to methylene chloride is possible, however, as trace amounts of methylene chloride were produced from chloroform. Trace amounts of ethane observed in chloroform transformation also indicate that the dichloromethyl radical may form. The lower reactivity of chloroform relative to CT may reflect the increased carbon−halogen bond dissociation energy, 73 kcal/mol for $CHCl_3$ vs 67.9 kcal/mol for CCl_4 (*18*). Additionally, the lack of C2 and C3 coupling products may be because formation of the dichloromethyl radical ($HCl_2C^{\bullet}$) from $CHCl_3$ is less thermodynamically favorable than formation of the trichloromethyl ($Cl_3C^{\bullet}$) radical from CCl_4 (*26*). The carbon mass balance of 81% is less than the 92% mass balance achieved during CT transformation, which may be due to (i) adsorption of chloroform to the catalyst support as more catalyst was used in this system and chloroform is less reactive than the other compounds tested or (ii) formation of a nonvolatile reaction product which was not detected in the headspace samples, as nonvolatile products may form from hydrolysis reactions or radical coupling.

Based on the hypothesized reaction pathways, eqs 3−6 were used to model the pseudo-first-order transformation of CT using the Pd/Al catalyst.

$$-\frac{dC_{CT}}{dt} = (k_{10} + k_{11} + k_{12})C_{CT} \quad (3)$$

$$\frac{dC_{CF}}{dt} = (k_{12}C_{CT} - k_{13}C_{CF}) \quad (4)$$

$$\frac{dC_{ethane}}{dt} = k_{11}C_{CT} \quad (5)$$

$$\frac{dC_{methane}}{dt} = (k_{10}C_{CT} + k_{13}C_{CF}) \quad (6)$$

Different model alternatives were tested and rejected based on goodness of fit. Only CT, methane, ethane, and chloroform were considered, and the lost carbon mass (7%) was neglected because $k_{loss} < 0.005$ L g^{-1} min^{-1}. The model fit is shown as lines in Figure 4, and best fit values for individual rate constants are given in Table 4. Based on the fitted parameters, carbon tetrachloride transforms approximately 65% via direct conversion to methane as calculated by the selectivity ratio $k_{10}/(k_{10} + k_{11} + k_{12})$ and approximately 35% via formation of the trichloromethyl radical $(k_{11} + k_{12})/(k_{10} + k_{11} + k_{12})$.

Rapid dehalogenation rates and the absence of toxic intermediates or products, in most cases, indicate the potential of palladium catalysts for environmental or industrial applications. Crucial application considerations still remain, however, such as (i) groundwater matrix effects on catalyst activity and lifetime, (ii) hydrogen dosing requirements, (iii) competing substrates, and (iv) catalyst fouling and deactivation. Current research efforts are focused on these issues.

Acknowledgments

The authors also thank Professor Paul Roberts, LLNL researchers, and members of the Reinhard Research Group for their helpful insight and comments. Although the research described in this article has been funded in part by the United states Environmental Protection Agency through R825421-01-0 to Martin Reinhard, it has not been subject to the Agency's required peer and policy review and therefore does not necessarily reflect the views of the Agency, and no official endorsement should be inferred.

Literature Cited

(1) Schreier, C. G.; Reinhard, M. *Chemosphere* **1994**, *29*(8), 1743.
(2) Matheson, L. J.; Tratnyek, P. G. *Environ. Sci. Technol.* **1994**, *28*(12), 2045.
(3) Gillham, G. W.; O'Hannesin, S. F. *Ground Water* **1994**, *32*, 958.
(4) Lipczynska-Kochany, E.; et al. *Chemosphere* **1994**, *29*(7), 1477.
(5) Kovenklioglu, S. et al. *AIChE Journal* **1992**, *38*(7), 1003.
(6) Siantar, D.; et al. *Water Research* **1996**, *30*(10), 2315.
(7) Schreier, C. G.; Reinhard, M. *Chemosphere* **1995**, *31*(6), 3475.
(8) Muftikian, R.; et al. *Water Res.* **1995**, *29*(10), 2434.
(9) Schüth, C.; Reinhard, M. *Appl. Catal. B: Environ.* **1998**, *18*, 215.
(10) Rylander, P. N. *Organic Synthesis with noble metal catalysts*; Academic Press: New York, 1967.
(11) Rylander, P. N. *Catalytic hydrogenation in Organic Synthesis*; Academic Press: New York, 1979.
(12) Schreier, C. G. Ph.D. Dissertation, Stanford University, 1996.
(13) Burris, D. R.; et al. *Environ. Sci. Technol.* **1996**, *30*(10), 3047.
(14) Harriott, P. *AICHe J.* **1962**, *8*(93).
(15) Roberts, P.; Dandliker, P. *Environ. Sci. Technol.* **1983**, *17*(8), 484.
(16) Weisz, P., Prater, C. In *Advances in Catalysis VI*; Academic Press Inc.: New York, 1954; pp 143−196.
(17) Pintar, A.; et al. *Appl. Catal. B: Environ.* **1996**, *11*, 81.
(18) Bouwer, E. J.; Wright, J. P *J. Cont. Hydrol.* **1988**, *2*, 155.
(19) Freedman, D.; Gossett, J *Appl. Environ. Microbiol.* **1989**, *55*(11), 2144.
(20) Orth, W. S.; Gillham, R. W. *Environ. Sci. Technol.* **1996**, *30*(1), 66.
(21) Crisafulli, C.; et al. *J. Mol. Catal.* **1989**, *50*(1), 67.
(22) Holgado, M. J.; Rives, V. *J. Mol. Catal.* **1989**, *53*(3), 407.
(23) Criddle, C. S.; McCarty, P. L. *Environ. Sci. Technol.* **1991**, *25*(5), 973.
(24) Kriegman-King, M. R.; Reinhard, M. *Environ. Sci. Technol.* **1994**, *28*(4), 692.
(25) Kriegman-King, M. R.; Reinhard. M., *Environ. Sci. Technol.* **1992**, *26*(11), 2198.
(26) Reinhard, M.; et al. In *Subsurface Restoration*; Ward, C., Cherry, J., Scalf, M., Ed.; Ann Arbor Press: Chelsea, MI, 1997; pp 397−409.

Received for review September 18, 1998. Revised manuscript received February 24, 1999. Accepted March 1, 1999.

ES980963M